International Journal of Entomology Research
www.entomologyjournals.com
ISSN: 2455-4758
Received: 08-03-2026, Accepted: 08-04-2026, Published: 23-04-2026
Volume 11, Issue 2, 2026, Page No. 146-156

Reduced expression of acid ceramidase-1 (*asah-1*) alters fecundity, lifespan and lipid levels in *Caenorhabditis elegans* mitochondrial mutants

Nikhita Deka[1,2], Lipika Khataniar[3], Roshan Sarmah[4], Aiswarya Baruah[5*]
[1] DBT-NECAB, Assam Agricultural University, Jorhat, Assam, India
[2] Department of Life Sciences, Dibrugarh University, Dibrugarh, Assam, India
[3] Department of Biotechnology, The Assam Kaziranga University, Jorhat, Assam, India
[4] Department of Botany, Debraj Roy College, Golaghat, Assam, India
[5] Department of Plant Breeding and Genetics, Biswanath College of Agriculture, AAU, Biswanath Chariali, Assam, India
Correspondence Author: Aiswarya Baruah

Abstract
In *Caenorhabditis elegans*, RNAi-mediated knockdown and other genetic mutations in the mitochondrial electron transport chain (ETC) have revealed the molecular basis of lifespan and developmental outcomes associated with mitochondrial dysfunction. An important transcription factor, CEP-1, a homolog of mammalian p53, regulates longevity in ETC mutants in response to mitochondrial stress and differentially regulates a few genes depending on the ETC mutations. Out of these, a gene, *asah-1*, encoding N-acylsphingosine amidohydrolase 1, is an ortholog of human asah1, which is important in sphingolipid and fatty acid metabolism and breaks down ceramide to sphingosine and fatty acid. In humans, mutations in this gene are associated with diseases such as sphingolipidosis and Farber lipogranulomatosis. Here, we show the physiological relevance of knocking down *asah-1* in *C. elegans* wild-type and mitochondrial mutants, *isp-1(qm150)* and *gas-1(fc21),* by investigating its effects on lifespan, reproduction, gene expression, development and overall body lipid levels. This has provided new insights into the functional relevance of *asah-1* in metabolism and physiology in *C. elegans*.

Keywords: *Caenorhabditis elegans*, *asah-1*, RNA Interference, mitochondrial electron transport chain dysfunction

Introduction

Dynamic, double-membraned mitochondria govern energy metabolism, redox balancing, and apoptosis. The ETC (Electron Transport Chain) consists of four multi-subunit complexes (I-IV) and ATP synthase, also known as Complex V. It facilitates electron transport from NADH and $FADH_2$ to molecular oxygen, coupling proton translocation and ATP synthesis, collectively known as oxidative phosphorylation (OXPHOS) (Spinelli & Haigis, 2018 [25]). Recent research links mitochondria-derived damage-associated molecular patterns (DAMPs) to chronic inflammation, which is called "inflammaging" or a hallmark of ageing (West & Shadel, 2017 [34]). Age-related diseases include cardiovascular disease, neurodegenerative disorders, and metabolic syndrome, which are linked to mitochondrial malfunction (Sun *et al*., 2016 [28]). Environmental pressures and genetic abnormalities influence electron transport chain functioning, ultimately impacting development, growth, and ageing. In addition, genetic as well as environmental factors can cause moderate to life-threatening symptoms by hampering mitochondrial activity. It is unclear how varying degrees of mitochondrial malfunction affect longevity. Model animals, including *Drosophila melanogaster* (Rana *et al*., 2017 [22]), the nematode, *Caenorhabditis elegans* (Xu *et al*., 2018 [35]), and mice (Wang *et al*., 2015 [33]) have illuminated mitochondrial dynamics, genetics and bioenergetics, helping us understand mitochondrial dysfunction and its impact on ageing and physiology.

The nematode *C. elegans* is a powerful model for studying mitochondrial dysfunction-induced cellular and organismal alterations (Lee *et al*., 2003 [15]). ETC mutations in *C. elegans* have been found to result in long and short lives. The *nuo-6(qm200)* mutant, which has a point mutation in complex I's NADH-ubiquinone oxidoreductase, the *isp-1(qm150)* mutant, which has a point mutation in complex III's Rieske iron sulphur subunit, and the *clk-1(e2519)* mutant, which has a coenzyme Q biosynthesis enzyme mutation, all show prolonged lifespans (Feng *et al*., 2001 [7]; Yang & Hekimi, 2010 [36]). However, the *mev-1(kn-1)* mutant and the *gas-1(fc21)* mutant, which have point mutations in the succinate dehydrogenase subunit c of complex II and complex I's NADH: ubiquinone oxidoreductase NDUFS2 subunit, respectively, live much shorter than wild-type worms (Kondo *et al*., 2005 [14]). Genetic mutations and RNAi-mediated suppression of ETC subunits in worms are revealing the molecular underpinnings of mitochondrial dysfunction-associated lifespan. For instance, RNAi and candidate screens have discovered transcription factors like CEH-23 (Walter *et al*., 2011 [31]), CEP-1 (Torgovnick *et al*., 2010 [29]) and TAF-4 (Khan *et al*., 2013 [11]) that regulate ETC mutant longevity. Earlier data have indicated that mutations in the *C. elegans* ETC subunit *isp-1* engage CEP-1 in initiating a stress response that results in a longer lifespan. Conversely, mitochondrial defects, due to mutations in the ETC subunit *gas-1*, act through CEP-1 to confer a shorter lifespan. Thus, CEP-1 affects longevity differently depending on mitochondrial stress, though the mechanism behind CEP-1's fascinating duality is unknown (Torgovnick *et al*., 2010 [29]; Baruah *et al*., 2014 [1]).

CEP-1 (*C. elegans* p53-like protein-1) in *C. elegans* is a homolog of the p53 family in mammals, making it a more accessible model for investigating the various roles of p53. The tumour suppressor gene p53 is a pivotal regulator of cellular metabolic equilibrium. In addition to its established roles in cell cycle arrest and apoptosis, p53 actively

responds to mitochondrial stress and exhibits a dual function; mild stress prompts p53 to facilitate cellular repair and activate antioxidant systems, whereas more severe stress triggers p53 to initiate apoptosis and senescence (Rufini *et al*., 2013 [23]). The dual function of p53 remains ambiguous; a potential explanation may lie in its dependency on the intensity and nature of stress, like that of *cep-1*. Prior investigations revealed that CEP-1 can differentially modulate a group of genes based on specific ETC mutations, as evidenced by the comparison of genome-wide expression profiles between long-lived and short-lived ETC mutants following *cep-1* removal (Baruah *et al*., 2014 [1]; Khataniar *et al*., 2024 [12]). The present study aimed to confirm one such gene, *asah-1*, which encodes N-acylsphingosine amidohydrolase 1 in *C. elegans* (K11D2.2). ASAH-1 codes for an acid ceramidase, which is responsible for the hydrolysis of ceramide to sphingosine and fatty acid (Li & Kim, 2022 [16]). This gene has been found to participate in fatty acid and sphingolipid metabolic processes and is essential for initiating a mitochondrial-to-cytosolic stress response (Kim *et al*., 2016 [13]). The human ortholog (ASAH-1) of this gene is associated with sphingolipidosis, Farber lipogranulomatosis and spinal muscular atrophy accompanied by progressive myoclonic epilepsy (Yu *et al*., 2018 [37]). In this study, two ETC mutants were used: long-lived *isp-1(qm150)* and short-lived *gas-1(fc21)* and we observed that RNAi-mediated depletion of *asah-1* dramatically affected the longevity of the *isp-1* mutant, but not the *gas-1* mutant. This finding corroborates our hypothesis that CEP-1 can selectively modulate a limited group of target genes to produce varied lifespan effects in response to mutations in different ETC components. Consequently, in the context of ETC dysfunction, we examined the impact of *asah-1* RNAi knockdown in *C. elegans*, utilising gene expression, lifespan analysis, fecundity assays, and lipid staining as endpoints, with *cep-1* in consideration, and the results provided insights into the functional significance of *asah-1* in physiology and regulation in *C. elegans*.

Materials and Methods

C. elegans strains used and growth conditions

N2 Bristol strain of *C. elegans* as wild-type, *cep-1(gk138)* strain, *isp-1(qm150)*, a long-lived ETC mutant, *cep-1(gk138);isp-1(qm150)* double mutant, *gas-1(fc21)*, a short-lived ETC mutant and *cep-1(gk138);gas-1(fc21)* double mutant, were all utilised in this study. The strains were collected from the National Institute of Immunology, New Delhi. All the *C. elegans* strains were grown and maintained at 20°C, in tissue culture plates (60mm or 100mm) containing nematode growth medium (NGM composition – Agar (17g/L), NaCl (3g/L), Peptone (2.5g/L), $CaCl_2$ (1mM), $MgSO_4$ (1mM), Potassium phosphate buffer (25mM) (pH 6.0), Cholesterol (5mg/L)), seeded with *Escherichia coli* OP50 bacteria as a food source (Brenner, 1974 [2]). *E. coli* OP50 bacteria were grown at 37°C and maintained using Luria Bertani (LB) (HiMedia) agar and broth. To conduct RNA-interference experiments, the *E. coli* strain HT115 (DE3) was used.

RNA Interference of *asah-1* via RNAi feeding

Nematode Growth Media (NGM) was supplemented with 50µg/ml ampicillin, 5µg/ml tetracycline and 1 mM IPTG (final concentration) to prepare RNAi plates, carrying *E. coli* HT115 transformed respectively with the empty L4440 plasmid (feeding vector) and the *asah-1* gene cloned into the L4440 plasmid. A single colony of bacteria was allowed to grow in Luria Bertani (LB) broth supplemented with 50µg/ml Ampicillin and 5µg/ml Tetracycline, overnight at 37˚C in a shaker incubator. The following day, after verifying OD values between 0.4 and 0.8, the bacterial culture was centrifuged at 5000 rpm and resuspended in fresh LB broth to achieve a 5-fold bacterial culture, which was subsequently inoculated onto the RNAi plates, left to dry, and kept overnight at room temperature for induction. To obtain a synchronized population, gravid adult worms were exposed to bleaching, which resulted in the production of closely synchronised embryos that were harvested by centrifugation. Such synchronized L1 larvae, obtained by the egg-prep method, were transferred to these RNAi plates to feed upon and followed up with the assays. Plates were made fresh before every experiment.

Quantitative reverse transcription PCR (qRT-PCR)

Quantitative real-time PCR was performed to confirm the knockdown of *asah-1* following RNA interference feeding in worms, and also, to compare the expression of other *cep-1* target genes after *asah-1* RNAi knockdown in respective worm strains. TRI reagent (Sigma) was utilised to extract total RNA from synchronized L4-stage worms. RNA purification and cDNA synthesis were performed utilising the PrimeScript™ RT reagent Kit (TaKaRa). The QuantStudio 3 Real-Time PCR System (Thermo Fisher Scientific) was used to assess gene expression via qRT-PCR, utilising TB Green® Premix Ex Taq™ II (Tli RNase H Plus) (TaKaRa). ΔΔCt technique was used for data analysis, with Actin (*act-1*) as the internal control. Each sample had three technical replicates, and the experiment was conducted three times.

Lifespan Assay

Lifespan experiments were carried out at 20°C. The embryos obtained after bleaching were transferred to NGM plates seeded with OP50 to grow to the L4 larval stage. To perform RNAi-mediated lifespan assays, 150 L4-stage larvae were transplanted to 60mm NGM RNAi plates, with each plate containing 30 worms (5 technical replicates). *E. coli* HT115 containing the empty L4440 plasmid was considered to be the control. Time (t=0) was established as the day of the worm transfer to the RNAi plates. Every day, plates were inspected, and worms were classified as dead or alive by repeatedly prodding them with a platinum wire worm pick. Worms that died from causes unrelated to ageing or those that got lost from the plates were referred to as 'censored'. This classification was considered in the statistical analysis. Survival analysis was done using the OASIS 2 online tool (https://sbi.postech.ac.kr/oasis2/), with the survival function estimated using the Kaplan-Meier method and the statistical analysis via the Mantel-Cox log-rank test (Han *et al*., 2016 [8]). The lifespan graphs were plotted with percentage survival on the Y-axis and the number of days on the X-axis. Lifespans were represented as average life span ± SEM.

Fecundity Assay

For fecundity measurement, 5 to 10 young adults were individually transferred onto fresh 35mm plates inoculated with HT115 bacteria with the empty L4440 vector and the

asah-1 RNAi clone, so that each plate contains a single worm. These were treated as the parent worms and were allowed to lay eggs. Incubation was done at 20°C, and parent worms were transferred to fresh plates every 12 hours till egg laying ceased, and also to prevent overcrowding of the plates. The progeny yield on each plate was quantified after 36 hours of removing the parent worm. The average brood size for each strain was compared using Student's t-test.

Development Assay

The developmental period of mutant worms was compared by introducing 3 to 5 gravid adult worms onto fresh plates inoculated with HT115 bacteria harbouring the empty L4440 vector (control) and the *asah-1* RNAi clone, allowing the worms to lay eggs at 20°C. After 6 hours, adult worms were removed from the plates, allowing the eggs to hatch. The developmental stages of all test worms were assessed daily using a dissecting microscope. Approximately 40 worms of each worm strain were placed on agar pads and examined under a compound microscope. The developmental stages of the worms were observed, measured, and the average percentage was used to plot graphs. Five technical replicates were used to calculate the average for each worm type.

Lipid Staining of *C. elegans* using Nile Red dye

To measure lipid levels, Nile Red (NR) dye was used, following the staining protocol by Escorcia *et al*. (2018) [6]. Developmentally synchronous worm population grown on L4440 control and *asah-1* RNAi plates was fixed with 40% isopropanol. Fixed worms were stained with Nile Red dye for 2 hours in the dark, then destained with PBST (Phosphate-buffered saline) for 30 minutes in the dark. 5µL of worm suspension was placed on a microscope slide and covered with a coverslip for imaging. A Leica TCS SPE Confocal laser scanning microscope was used for imaging. Images of Nile Red-stained worms were acquired using the GFP channel provided in the Las X software, keeping the same conditions for all the strains. Image analysis was done using ImageJ software, followed by statistical analysis.

Lipid Staining using Oil Red O dye

To monitor lipid distribution, Oil Red O (ORO) dye was used to stain lipids (Escorcia *et al*., 2018 [6]). Synchronised population of worm strains were obtained by bleaching and allowed to grow on L4440 (control) as well as *asah-1* RNAi NGM plates. Worms were fixed using 40% isopropanol and incubated in a rocker. ORO dye working solution was added to worms, followed by rotation at 30 rpm for 2 hours at room temperature. This was followed by destaining of the worm samples using PBST for 30 minutes at 30 rpm. These were then centrifuged, and a small amount of supernatant was kept to obtain a worm suspension, from which 5µL was put on a microscope slide and covered with a coverslip for viewing under the microscope. A binocular microscope (Carl Zeiss) with attached camera (Axiom 105 color) was used for imaging. Images were saved using the ZEN 2 software, and analysis was performed using ImageJ.

Image Acquisition and Analysis

For viewing under the microscope, *C. elegans* were mounted on agarose pads prepared with 2% agarose in M9 solution, on glass microscope slides. (M9 buffer composition in 1L Milli Q water – KH_2PO_4 (2g), Na_2HPO_4 (6g), and NaCl (5g); 1M $MgSO_4$ (1ml) added after autoclaving). Ten to fifteen worms from each plate were picked onto the agarose pad and immobilised using 1 mM Levamisole (Sigma-Aldrich). All the image analyses were done using the ImageJ software (Schindelin *et al*., 2012 [24]). The Polygon selection tool was used to outline the imaged worms, and the Measure function was then invoked in the Analyze pull-down menu. This will calculate the Gross fluorescence (IntDen) and the total worm area for each worm. To account for any autofluorescence in the image, five background measurements were also taken using the Oval tool, and the average background fluorescence intensity was calculated. This was subtracted from each imaged worm by using the formula:

Net fluorescence (N) = Gross fluorescence (G) – (Total worm area (A) X Average background fluorescence (B))

From this, the fluorescence intensity, which is expressed in arbitrary units (a.u.), was calculated by normalizing by worm size, using the following formula:

Fluorescence Intensity = Net fluorescence (N) / Total worm area (A)

Statistical Analysis

For each experiment, at least three biological replicates had been performed, except otherwise stated in the figure legends. Microsoft Excel was used to generate graphs, and the p-values were calculated using a two-tailed t-test.

Results

Distinct expression of *asah-1* in *isp-1* and *gas-1* and its knockdown in wild-type and the ETC mutants:

Among the limited number of CEP-1-regulated genes potentially influencing the dual effects of CEP-1 in mitochondrial mutants with differing dysfunction levels, the expression of *asah-1*, which encodes the *C. elegans* homolog of ceramidase, was checked in the mitochondrial mutants via qRT-PCR. Expression of *asah-1* was found to be downregulated in the *cep-1* mutant and significantly upregulated in the *isp-1* mutant (p=0.0006) relative to the wild-type. The *cep-1;isp-1* double mutant exhibited a comparable reduction in *asah-1* expression (p=0.01) to that of the *cep-1* mutant (Figure 1). Interestingly, *asah-1* was slightly induced in the short-lived *gas-1* mutant (p=0.01) independently of *cep-1*.

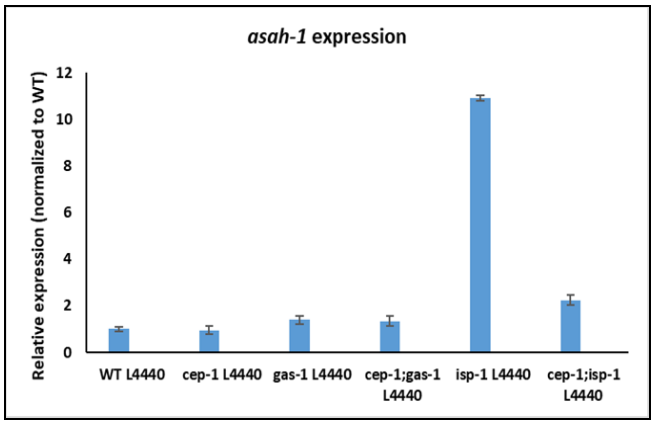

Fig 1: qRT-PCR results showing *asah-1* expression levels in WT and mitochondrial ETC mutants. Error bars represent standard errors

Following this, RNA interference-mediated knockdown of *asah-1* was executed in the *C. elegans* strains, as detailed in the materials and methods section. The expression levels of *asah-1* in wild-type and mitochondrial mutants, following exposure to *E. coli* HT115 harbouring the empty plasmid pL4440 (control) and with double-stranded RNA targeting *asah-1* (*asah-1* RNAi), were compared by qPCR, revealing a knockdown of the gene (Figure 2). Upon confirmation of knockdown, its impact on longevity, development, reproduction, and lipid levels in wild-type and mutant organisms was assessed.

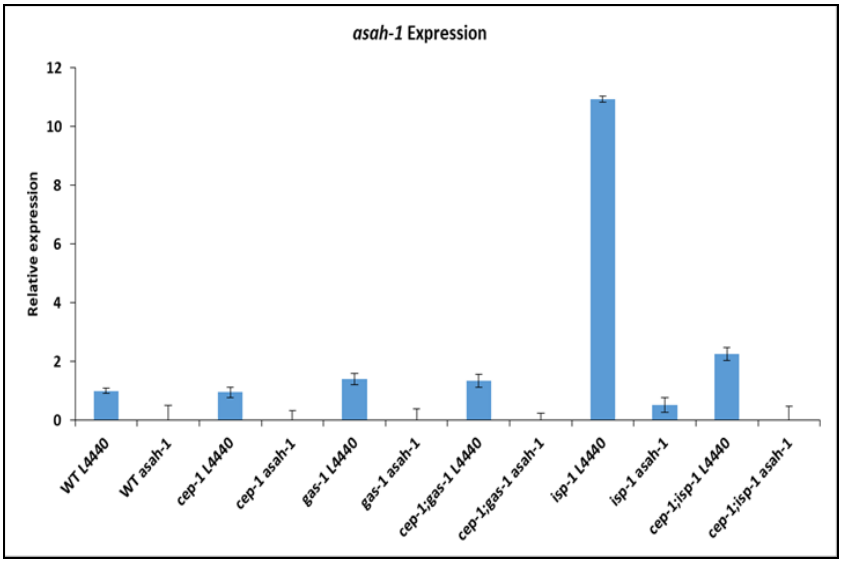

Fig 2: RNAi-mediated knockdown of *asah-1* in wild-type, *cep-1*, *isp-1*, *cep-1;isp-1*, *gas-1* and *cep-1;gas-1* mutants. Error bars represent standard errors

Asah-1 exerts distinct longevity outcomes in *isp-1* and *gas-1* mutants

To evaluate if *asah-1* overexpression enhanced the longevity of *isp-1* mutants, we analysed the lifespans of *isp-1* and *cep-1;isp-1* mutants following its knockdown via RNA interference. Wild-type worms lived 22.5 ± 0.5 days, which reduced to 16.3 ± 0.6 days (p=0) (Mantel-Cox test) after *asah-1* knockdown. The *cep-1* mutant worms lived 23.86 ± 0.7 days, which again reduced to 18.16 ± 0.5 days (p <0.00001) upon *asah-1* knockdown. The mitochondrial mutant *isp-1* lived 27.74 ± 0.85 days. The RNAi-induced knockdown of *asah-1* markedly diminished the prolonged longevity of *isp-1* mutants to 13.6 ± 0.66 days (p=0), surpassing the effect of *cep-1* inactivation, showing 20.55 ± 0.59 days. Notably, *asah-1* RNAi further diminished the lifetime of the *cep-1;isp-1* double mutant to 12.16 ± 0.45 days (p=0), indicating that *cep-1* and *asah-1* do not function within the same genetic pathway to regulate *isp-1* longevity (Figure 3A). We further examined whether *asah-1* is universally essential for the survival of the *gas-1(fc21)* mutant. The *gas-1* mutants exhibited a lifespan of 16.87 ± 0.42 days. The observation that *asah-1* suppression did not influence the longevity of the *gas-1* mutant (16.56 ± 0.58 days) was noteworthy. The deletion of *cep-1* ameliorated the transient phenotype of the *gas-1* mutant (18.56 ± 0.57 days), indicating that CEP-1 plays a critical role in the lifespan effects of the *gas-1* ETC mutant. The knockdown of *asah-1* in *cep-1;gas-1* resulted in reduced longevity (12.68 ± 0.48 days), demonstrating a distinct effect compared to *cep-1* inactivation (Figure 3).

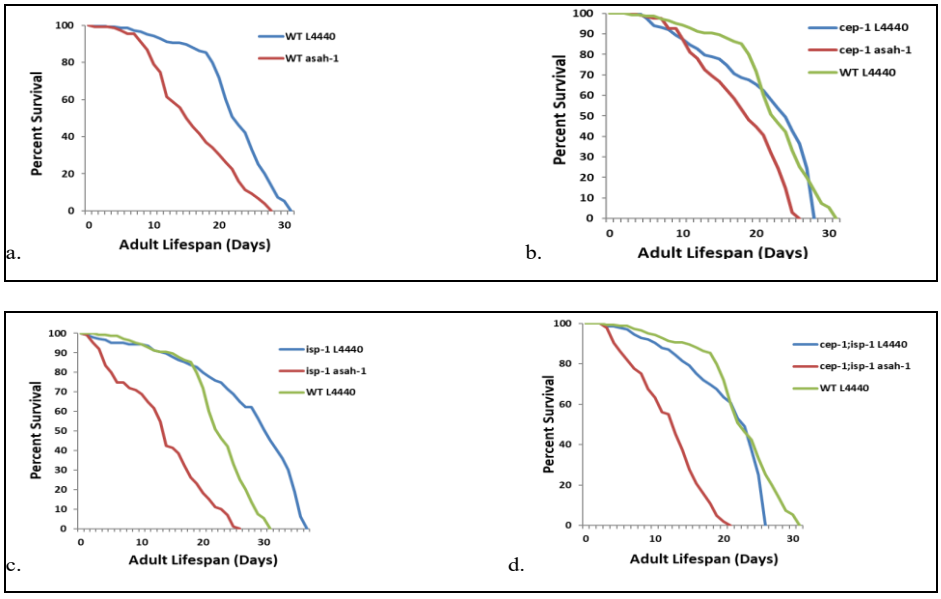

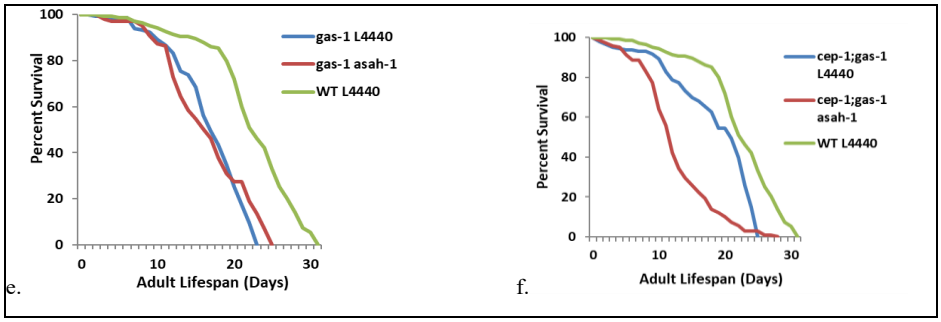

Fig 3: Survival curves showing lifespans of *C. elegans* mutants at 20°C after RNAi-mediated knockdown of *asah-1* as compared to wild-type N2 (Bristol stock) as the control

***Asah-1* knockdown reduces brood size in *isp-1* and *gas-1* mutants:** To examine the potential regulatory role of CEP-1 on *asah-1* on the reproductive capacity of the mitochondrial ETC mutants, the mean brood size of *isp-1* and *gas-1* mutants, with and without *cep-1*, was assessed in relation to that of wild-type worms, upon *asah-1* knockdown. The brood size of the *cep-1* mutant did not differ significantly from the wild-type, but the mitochondrial mutants *isp-1* and *gas-1* exhibited significantly reduced brood sizes relative to the wild-type worms ($p<0.0001$). The average brood size of wild-type worms did not differ significantly after *asah-1* RNAi knockdown. The *cep-1* mutant displayed a slightly increased brood size after *asah-1* knockdown. Also, after *asah-1* knockdown, the average brood size of *isp-1* ($p=0.00001$) and *gas-1* ($p<0.0001$) mutant worms decreased significantly compared to wild-type. In comparison to the *isp-1* and *gas-1* single mutants, the double mutants, *cep-1;isp-1* and *cep-1;gas-1* showed a further reduction in brood size, respectively ($p<0.05$) (Figure 4). These suggest that the reproductive defect related to mitochondrial dysfunction worsens by *cep-1* loss. Importantly, knockdown of *asah-1* in both *cep-1;isp-1* and *cep-1;gas-1* increased the average brood size. However, the increase in *cep-1;isp-1* was greater than wild-type ($p=0.03$).

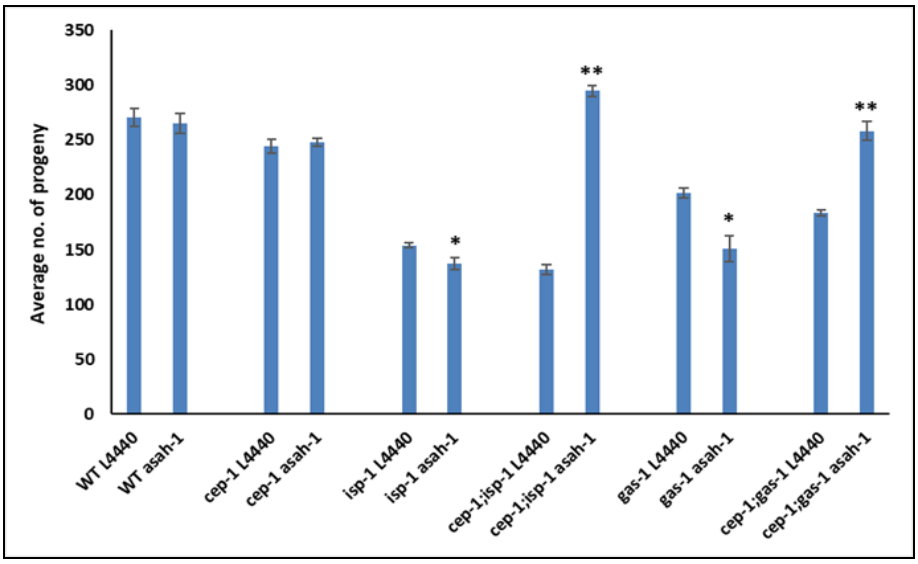

Fig 4: Average number of progeny production for *C. elegans* wild-type and mutants after *asah-1* RNAi treatment at 20°C (*$p<0.05$, **$p<0.0005$)

Varying development outcomes in ETC mutants

To evaluate the significance of CEP-1 control of *asah-1* in the development of ETC mutants, the developmental duration of *isp-1* and *gas-1* mutants, with and without *cep-1*, was compared to that of wild-type worms following *asah-1* RNAi knockdown. The data indicated that wild-type and *cep-1* mutants exhibited comparable developmental rates. At 65 hours post egg lay, all wild-type worms reached adulthood (100%). The *cep-1* mutant developed slightly slower, and about 90% of its population reached adulthood at 65 hours. Knockdown of *asah-1* reduced the development time of both wild-type and *cep-1* worms, with worms in the L3 (25%), L4 (75%) and L3 (22%), L4 (70%), YA (8%) stages at 65 hours, respectively. The *isp-1* mutant worms showed a typical "Mit" (Mitochondrial mutant) phenotype with delayed growth in the L1 (18%), L2 (78%), and L3 (4%) stages after 65 hours. Knockdown of *asah-1* improved this slow development, shifting the early larval stages in *isp-1* mutants to L2 (12%), L3 (68%) and L4 (20%) stages. This observation was similar to *cep-1* inactivation in *isp-1* worms, as *cep-1;isp-1* double mutant worms were found to be in the L2 (12%), L3 (40%), L4 (38%) and YA (10%) stages at 65 hours. Furthermore, *asah-1* knockdown exerted no additional impact on its development. The *gas-1* mutants exhibited accelerated development, with the majority of *gas-1* mutants in the L4 (6%) and YA (93%) stages after 65 hours. The knockdown of *asah-1* marginally postponed this progression. Notably, inactivating *cep-1* also postponed the growth of *gas-1* mutants. The *cep-1;gas-1* double mutants were in the L3 (7%), L4 (8%), and YA (85%) stages after 65 hours. However, *asah-1* knockdown had no further effect on its development (Figure 5).

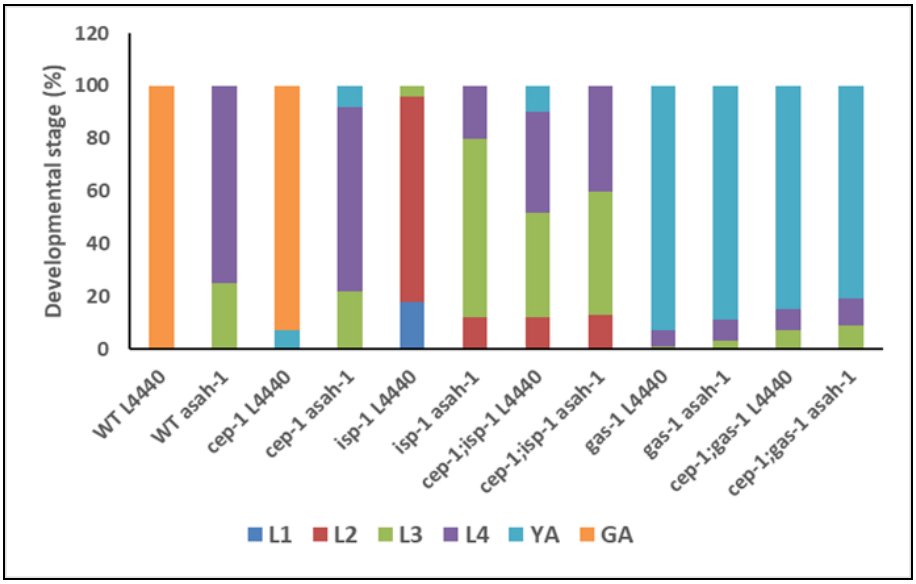

Fig 5: Percentage of worms at each developmental stage (after RNAi-mediated knockdown of *asah-1*) after 60 hr of growth from the embryonic stage at 20°C

Context-dependent effects of *asah-1* knockdown on lipid levels:

Significant differences in body lipid levels were observed in all mitochondrial mutant strains under control conditions compared to wild-type control worms (Figure 6A). Lipid accumulation was quantified using the Nile Red staining assay and reported as fluorescence intensity after imaging and processing (Figure 6B). We found that the average fluorescence intensity did not differ significantly between wild-type and *cep-1*. The average fluorescence intensity significantly increased in the *isp-1* mutant ($p<0.001$), whereas, it decreased in the *cep-1;isp-1* double mutant, indicating CEP-1-dependent suppression in body lipid levels in the *isp-1* mutant (Khataniar *et al*., 2024 [12]). Knockdown of *asah-1* resulted in significant decrease in lipid levels in *cep-1* ($p=0.0001$) and *cep-1;isp-1* ($p=0.00001$) mutants compared to respective controls. The average fluorescence intensity significantly decreased in the *gas-1* mutant ($p<0.0001$), which decreased further in the *cep-1;gas-1* double mutant ($p<0.0001$). Knockdown of *asah-1* significantly increased lipid levels in the *gas-1* mutant ($p=0.001$) compared to its control

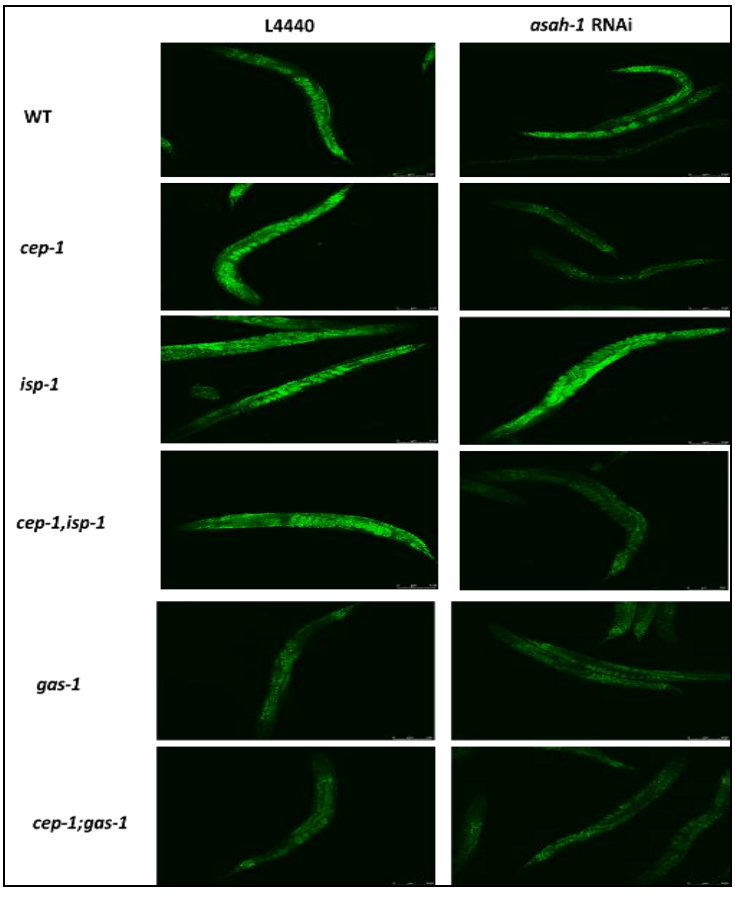

Fig 6A: Representative images showing Nile Red staining of *C. elegans* mutants at 20°C after RNAi-mediated knockdown of *asah-1*

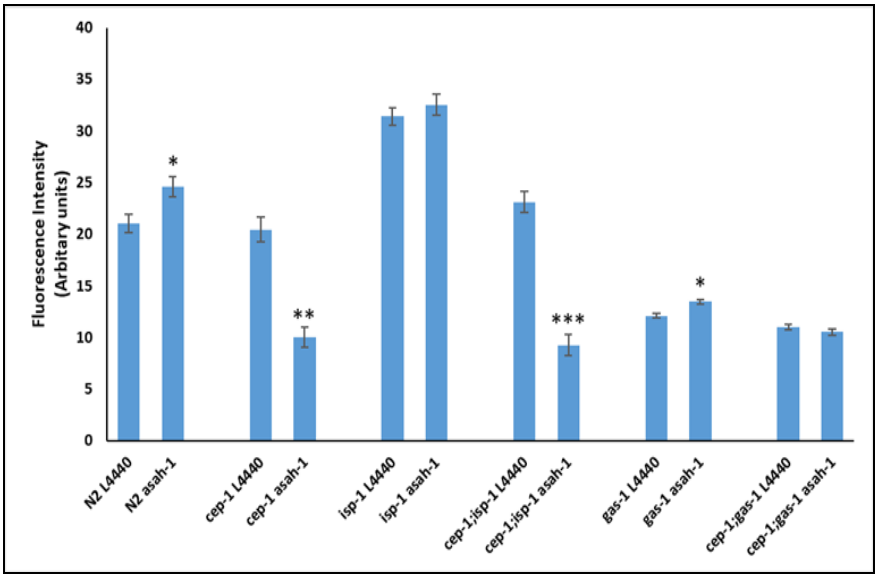

Fig 6B: Graphs showing overall lipid levels in worms at 20°C after *asah-1* knockdown

Knockdown of *asah-1* increases ORO signals in *isp-1* and *gas-1*: Significant differences in lipid staining were observed in the mitochondrial mutants compared to wild-type control worms (Figure 7A). Here, lipid storage and distribution were quantified using the Oil Red O (ORO) staining assay (Figure 7B). The average ORO signal in wild-type and in *cep-1* differed significantly (p=0). This signal decreased in wild-type after *asah-1* knockdown (p=0). The average ORO signal significantly increased in the *isp-1* mutant (p=0.00002); and slightly changed in the *cep-1;isp-1* double mutant, compared to wild-type. Also, compared to the wild-type, the average ORO signal significantly decreased in the *gas-1* mutant (p=0.0007); and increased in the *cep-1;gas-1* double mutant. So, inactivation of *cep-1* altered lipid storage in the *isp-1* and *gas-1* mutants. Knockdown of *asah-1* resulted in a decrease in lipid levels in the wild-type (p=0), *cep-1* (p=0.000006), *cep-1;isp-1* (p<0.0001) and *cep-1;gas-1* (p=0.0250) mutants, and an increase in *isp-1* (p=0.0011) and *gas-1* (p=0.0023) mutants, compared to their respective controls.

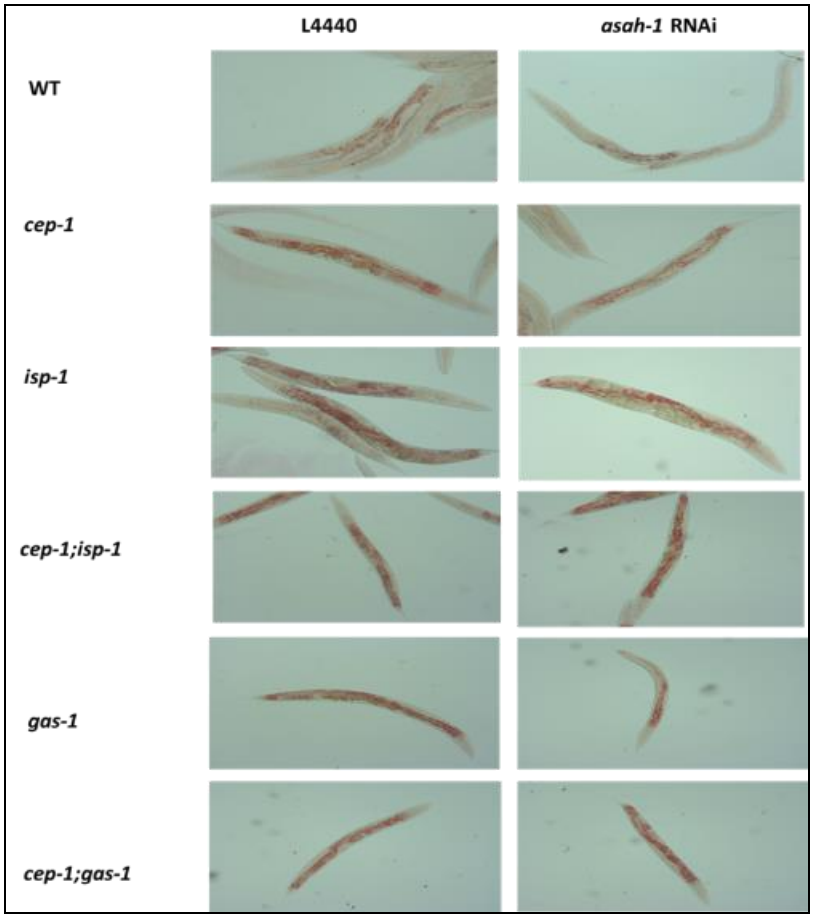

Figure 7A: Representative images showing Oil Red O staining of *C. elegans* mutants at 20°C after RNAi-mediated knockdown of *asah-1*

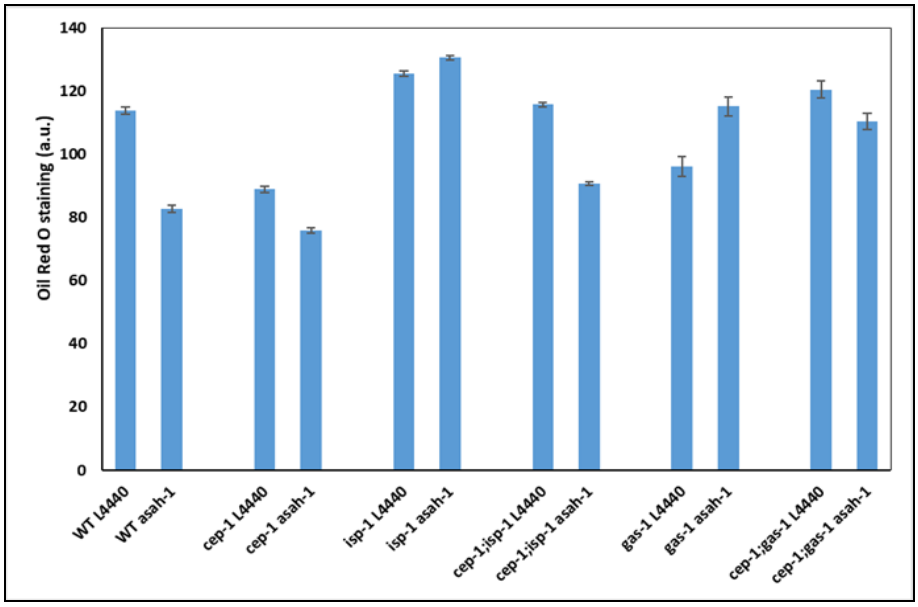

Fig 7B: Graphs showing Oil Red O staining intensities in worms after knockdown of *asah-1*

***Cep-1*-dependent change in expression of target genes in *isp-1* mutant**

To determine the involvement of *asah-1* in regulating the expression of other genes involved in fatty acid biosynthesis and ROS detoxification, expression levels of a few important genes such as ferritin-1 (*ftn-1*), superoxide dismutase (*sod-3*), fatty acid desaturase (*fat-2*) and fatty acid synthase (*fasn-1*), in the worms with and without knockdown of *asah-1* were evaluated. The qPCR analysis revealed increased expression of all the above-mentioned genes in the *isp-1* mutant, which decreased drastically in the *cep-1;isp-1* double mutant. There were marginal differences in the expression of these genes in the *gas-1* mutant after *asah-1* knockdown (Figure 8).

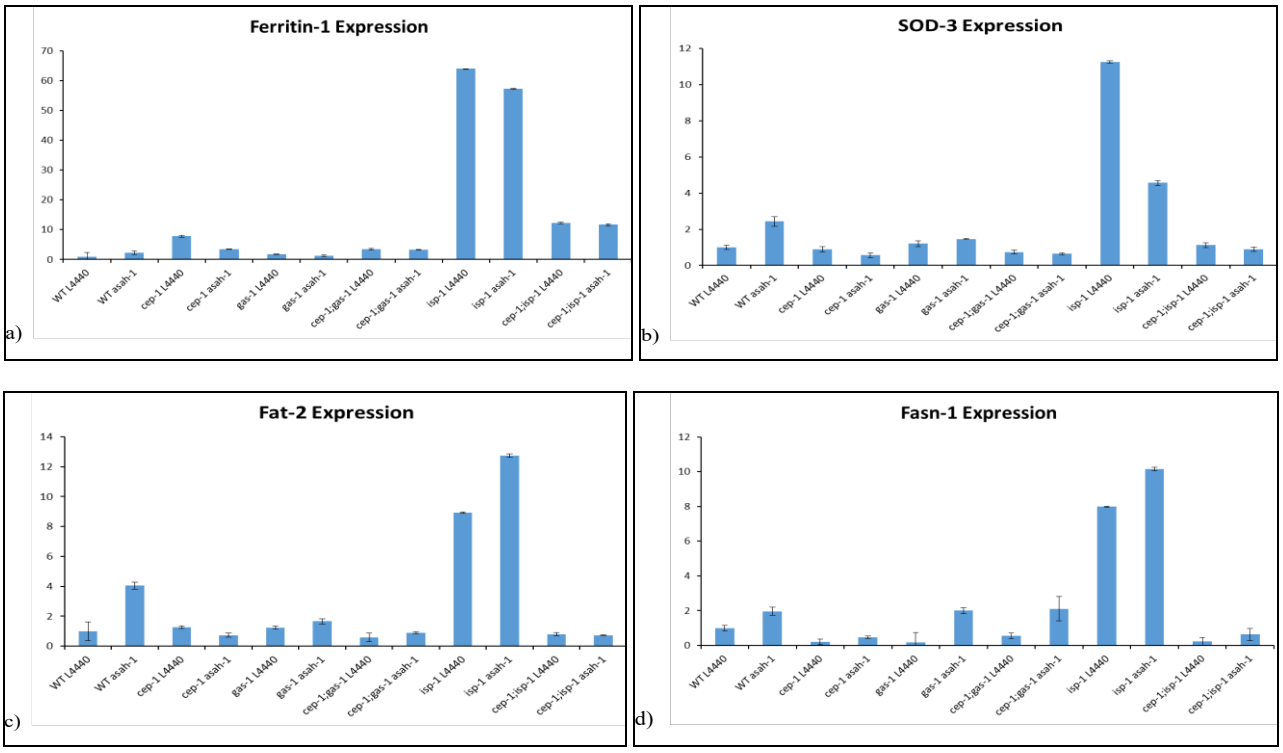

Fig 8: Expression of CEP-1 targets after *asah-1* knockdown

Discussion

The major function of p53/CEP-1 is to integrate stress signals and to orchestrate appropriate cellular responses. The finding that *asah-1* is upregulated in the *isp-1* long-lived mutant indicates that activation of this gene by CEP-1 led to metabolic reprogramming and increased stress resilience, a feature associated with increased lifespan. Our observations suggest that CEP-1 controls *asah-1* in wild-type and *isp-1* mutants, but is nonessential in the *gas-1* mutant. These results again align with recent work indicating that CEP-1 regulates a group of genes involved in longevity and mitochondrial stress adaptation (Zhi *et al.*, 2022 [38]). The complete knockdown of our gene of interest, *asah-1*, in the *C. elegans* strains demonstrates the efficacy

of the RNAi feeding method and supports the validity of the subsequent phenotypic investigation. This method ensures that the biological traits observed can be credited to *asah-1* knockdown, instead of any strain-specific or off-target variations. So, validation of knockdown provides a well-grounded basis for subsequent functional analysis (Deka *et al*., 2026 [4]). This helps to derive verified conclusions about the role of *asah-1* and its association with *cep-1* in varied worm genetic backgrounds. *Asah-1* is a modulator in lipid and sphingolipid metabolism. Given that lipid homeostasis significantly influences mitochondrial dysfunction, we aimed to examine whether *asah-1* regulation accounted for the roles of CEP-1 in the longevity of mitochondrial ETC mutants. In all the genetic backgrounds tested, *asah-1* RNAi knockdown shortened lifespan in adult worms, most remarkably in the case of the long-lived *isp-1* mitochondrial mutant (From 27.74 days to 13.6 days). So, *isp-1* longevity, which is accompanied by altered signalling or higher mitochondrial ROS levels, can be put down by disturbances in other mitochondrial regulators. This type of pattern is in line with concepts of mitochondrial-ageing-related work, as partial ETC dysfunction brings out adaptive stress responses that extend lifespan; however, these responses are eliminated or become lethal in the case of higher ETC stress (Cheng *et al*., 2023 [3]). For instance, RNAi of the *asah-1* gene was reported to partially reduce the extended lifespan of *daf-2* mutants (Murphy *et al*., 2003 [21]). Thus, the finding that knockdown of *asah-1* drastically reduces *isp-1* longevity depicts that ASAH-1 either participates in the stress-response program or adjusts to the altered bioenergetic state of *isp-1* mutants. Additionally, in agreement with our expression results indicating that *asah-1* is only slightly modulated by CEP-1 in the *gas-1* mutant, the lifetime of the *gas-1* mutant remained unaltered by *asah-1* knockdown.

Mitochondrial ETC mutants exhibit delayed development and diminished brood sizes, as well as alterations in lifespan (Feng *et al*., 2001[7]; Kayser *et al*., 2001 [10]). The brood size assay exhibited variation and interchange. Consistent with several mitochondrial mutants that trade reproduction for stress resistance or longevity, the *isp-1* and *gas-1* mitochondrial mutants also showed greatly reduced brood size as compared to the wild-type worms. Furthermore, knockdown of *asah-1* further increased *cep-1;isp-1* and *cep-1;gas-1* progeny number, implying *cep-1*'s potential significance in reproduction might be independent of that of *asah-1* in *isp-1* and *gas-1* mutants. This suggests that ASAH-1 contributes to energy metabolism or germline integrity under mitochondrial stress. But loss of *cep-1* may reconstruct signalling or resource allocation so that knockdown of *asah-1* moves the equilibrium back to reproduction. These kinds of background-specific effects have been documented previously. It has been shown that fecundity often decreases in mitochondrial mutants, similar to this case; however, multiple factors or regulators can interact to give rise to opposite outcomes. For example, UPRmt and ROS-linked pathways are associated with decreased fecundity in mitochondrial mutants, which can either be restored or suppressed further by genetic or environmental alteration (Dues *et al*., 2017 [5]). Our data obtained on the development timing of worms provides an additional aspect to the lifespan outcomes. When under mitochondrial stress (*isp-1* and *gas-1* mutants), *asah-1* knockdown showed accelerated and decelerated development, respectively, except when *cep-1* is inactivated, suggesting that *cep-1* and *asah-1* interact genetically for development, specifically. It indicates the influential role of ASAH-1 on the development rate, which again gets masked in the absence of *cep-1*. This could also imply metabolic compensation or changes in mitochondrial stress signalling, such as ROS, altered lipid homeostasis, which influence development. Prior studies have also shown that impairment in mitochondrial function produces a small body size and delayed development, and that the timing of development is responsive to mitochondrial impairments and to stress-responsive genes, specifically (Maglioni *et al*., 2019 [19]). Consequently, whereas both *asah-1* and *cep-1* collectively influence the development of the *isp-1* and *gas-1* mutants, the outcomes differ, indicating that their function in development varies among these mutants.

Recent work has described the importance of lipid distribution similar to lipid accumulation (Lynn *et al*., 2015 [17]). Published work has acknowledged the method of ORO staining for lipid distribution (Escorcia *et al*., 2018 [6]; Stuhr *et al*., 2022 [27]). ORO staining primarily localizes to lipid droplets in the intestine and also accumulates in the somatic region. In our study, the *cep-1* mutants displayed lower levels of neutral lipids as compared to wild-type worms, which can be associated with CEP-1's stress-responsive properties. In wild-type, *asah-1* knockdown increased the lipid levels, which can be attributed to the decrease in the fatty acid pool upon loss of *asah-1*. Knockdown of *asah-1*, along with *cep-1* loss, likely merges stress responses, ultimately leading to a decrease in lipid levels. Cellular metabolism is often rewired during mitochondrial impairments, which leads to altered fatty-acid composition, shown by various mitochondrial mutants (Maciej, 2020 [18]). Our work shows increased lipid levels in the *isp-1* mutant, which increased modestly on *asah-1* knockdown, likely due to alterations in signalling that raised lipid levels as compensatory responses. Lipid levels in the *cep-1;isp1* double mutant were observed to be similar to those in the wild-type, which suggests that CEP-1 is needed for the lipid phenotype shown by *isp-1*. CEP-1 seems to mediate a portion of the downstream transcriptional rewiring of mitochondrial stress, which led to lipid accumulation. So, in the absence of *cep-1* in the *cep-1;isp-1* mutant, the ability of *isp-1* to increase storage through pathway upregulation is lost, thus bringing back lipid levels to wild-type. *Asah-1* acts independently or downstream of *cep-1* in this case, as its knockdown in the *cep-1;isp-1* background decreased the lipid levels to the level as in *asah-1* knockdown in the *cep-1* mutant. Irrespective of the status of *isp-1*, *asah-1* knockdown exerts the signalling effects after *cep-1* inactivation. This shows that *asah-1* regulates lipid levels by a biochemical pathway that acts in the *cep-1* null scenario. In the *gas-1* mutant, *asah-1* knockdown significantly increased lipid levels. So, *asah-1* exerts similar effects in both these mutants, independent of *cep-1*. Additionally, the distribution of fat stores, which is mostly in the intestinal area, was also altered in the mutants.

Mitochondrial dysfunction in the *isp-1* mutant has been seen to trigger metabolic changes that heighten antioxidant or detoxification defences and other metabolic enzymes (Mao *et al*., 2019 [20]). Additionally, the *gas-1* mutant expresses changed physiological phenotypes like increased ROS levels, increased dependence on ETC complex II to support metabolic homeostasis, and decreased OXPHOS capabilities

(Kayser *et al*., 2001 [10]). The qRT-PCR pattern obtained here shows similar responses in the form of increased expression of *fat-2*, *fasn-1*, *ftn-1* and *sod-3* genes in *isp-1* mutant. The clear reduction in expression of the genes in the case of *cep-1;isp-1* double mutants shows a major role of CEP-1 in the *isp-1*-specific transcriptional program, because in the absence of *cep-1*, the stress signalling couldn't maintain or increase the expression of the above-mentioned genes. So, ETC dysfunction triggers the elevation of mitochondrial ROS and stress responses and activation of transcription factors like *cep-1*/p53. These again lead to changes in metabolic gene expression for energy reallocation, such as activation of fatty acid synthesis (*fasn-1*) and desaturation enzymes (*fat-2*) and also, upregulation of antioxidant genes like *sod-3*. Similar work was done by Mao *et al*. (2019) [20], which shows that mitochondrial dysfunction activates extensive metabolic and detoxification programs. Studies also show the role of *cep-1*/p53 in communicating bioenergetic stress in mitochondria into varied longevity and transcriptional outcomes (Ventura *et al*., 2009 [30]). These transcriptional outcomes ultimately are shown in phenotypes as seen in this work. Upregulation of the *fat-2* and *fasn-1* genes in *isp-1* and *gas-1* mutants is consistent with increased lipid levels, as evidenced by lipid staining. Ferritin regulates iron storage and release. Upregulation of *sod-3* and *ftn-1* genes in the *isp-1* mutant is also consistent with increased ROS signalling and detoxification ability, as observed in mitochondrial mutants. Additionally, elevated expression of *sod-3* in *isp-1* worms also plays a part in oxidative stress resistance that is required for its longevity, as inducing antioxidants is included in the compensatory mechanism that promotes lifespan extension in ETC mutants like *isp-1*. All these elevated gene expressions in *isp-1* are reduced drastically when *cep-1* is inactivated, ultimately changing lifespan, development and fecundity outputs. Overall, we observed different patterns for how these genes responded to the absence of *cep-1* in the two mutants. The majority of genes that showed substantial *cep-1*-dependent induction in the *isp-1* mutant moderately changed when *cep-1* was depleted in the *gas-1* mutant.

In conclusion, the datasets from lifespan, development, and fecundity assays show a consistent scenario that ASAH-1 has a largely protective function for organismal fitness and produces context-specific phenotypes, while exposing the effects of mitochondrial electron transport chain dysfunction upon its loss. Here, increased brood size and reduced lifespan after *asah-1* knockdown in *cep-1;isp-1* and *cep-1;gas-1* show that *asah-1* maintains longevity as well as brood size independently of *cep-1*. Also, *asah-1* and *cep-1* may act in the same genetic pathway to mediate the development time in *isp-1* and *gas-1* mutants. Lipid metabolism also affects cell and physiological functions that mediate animal lifespan (Staab *et al*., 2023 [26]). Here, *cep-1* loss is found to alter metabolic gene expression and contribute to maintaining lipid levels under control conditions. In *C. elegans*, sphingolipid homeostasis is critical, as inappropriate *asah-1* expression in neurons causes defects in the development of the nervous system (Wang *et al*., 2023 [32]). In this study, lipid homeostasis might be a determinant of *isp-1* longevity, but it does not appear to be important for mediating the lifespan of *gas-1* mutants. Additionally, *asah-1* was not induced in the *gas-1* mutant, another indication that the *gas-1* mutant might engage a different mechanism to extend lifespan. Reduced reproduction is associated with increased fat storage and prolonged life span in multiple organisms (Hansen *et al*., 2013 [9]). In our study, reduced brood size in both mutants could be due to increased fat storage during *asah-1* knockdown, which may be one of the factors leading to the reproductive defect. Overall, the *asah-1* gene is found to be a key component in maintaining lipid homeostasis, which directly impacts the overall longevity and development of the organism. To clarify the pathway of action of these genes and to investigate the biochemical interactions between them, it is necessary to perform expression analysis and genetic interaction screenings in future work. The results of the present study may contribute to a better understanding of the physiological effects of *asah-1* knockdown in *C. elegans*.

References

1. Baruah A, Chang H, Hall M, Yuan J, Gordon S, Johnson E, *et al*. CEP-1, the Caenorhabditis elegans p53 homolog, mediates opposing longevity outcomes in mitochondrial electron transport chain mutants. PLoS genetics,2014:10(2):e1004097.
2. Brenner S. The genetics of Caenorhabditis elegans. Genetics,1974:77(1):71-94.
3. Cheng YW, Liu J, Finkel T. Mitohormesis. Cell metabolism,2023:35(11):1872-86.
4. Deka N, Baruah A, Gogoi D, Vardhan GS, Boruah P, Sarmah R, *et al*. Unravelling the functional role of PLRG-1 in development and lifespan in Caenorhabditis elegans. InData-Driven AI: A Multidisciplinary Approach, 22-26.
5. Dues DJ, Schaar CE, Johnson BK, Bowman MJ, Winn ME, Senchuk MM, *et al*. Uncoupling of oxidative stress resistance and lifespan in long-lived isp-1 mitochondrial mutants in Caenorhabditis elegans. Free Radical Biology and Medicine,2017:108:362-73.
6. Escorcia W, Ruter DL, Nhan J, Curran SP. Quantification of lipid abundance and evaluation of lipid distribution in Caenorhabditis elegans by nile red and oil red O staining. Journal of visualized experiments: JoVE,2018:(133):57352.
7. Feng J, Bussière F, Hekimi S. Mitochondrial electron transport is a key determinant of life span in Caenorhabditis elegans. Developmental cell,2001:1(5):633-44.
8. Han SK, Lee D, Lee H, Kim D, Son HG, Yang JS, *et al*. OASIS 2: online application for survival analysis 2 with features for the analysis of maximal lifespan and healthspan in aging research. Oncotarget,2016:7(35):56147.
9. Hansen M, Flatt T, Aguilaniu H. Reproduction, fat metabolism, and life span: what is the connection?. Cell metabolism,2013:17(1):10-9.
10. Kayser EB, Morgan PG, Hoppel CL, Sedensky MM. Mitochondrial expression and function of GAS-1 in Caenorhabditis elegans. Journal of Biological Chemistry,2001:276(23):20551-8.
11. Khan MH, Ligon M, Hussey LR, Hufnal B, Farber R, Munkácsy E, *et al*. TAF-4 is required for the life extension of isp-1, clk-1 and tpk-1 Mit mutants. Aging (Albany NY),2013:5(10):741.
12. Khataniar L, Deka N, Gogoi D, Sarmah R, Baruah A. Functional analysis of CEP-1/P53 targeted genes in

mitochondrial mutant of Caenorhabditis elegans. BIOINFOLET Учредители: Diva Enterprises Private Limited,2024:21(4):421-34.
13. Kim HE, Grant AR, Simic MS, Kohnz RA, Nomura DK, Durieux J, *et al*. Lipid biosynthesis coordinates a mitochondrial-to-cytosolic stress response. Cell,2016:166(6):1539-52.
14. Kondo M, Senoo-Matsuda N, Yanase S, Ishii T, Hartman PS, Ishii N. Effect of oxidative stress on translocation of DAF-16 in oxygen-sensitive mutants, mev-1 and gas-1 of Caenorhabditis elegans. Mechanisms of ageing and development,2005:126(6-7):637-41.
15. Lee SS, Lee RY, Fraser AG, Kamath RS, Ahringer J, Ruvkun GA. *et al*. systematic RNAi screen identifies a critical role for mitochondria in C. elegans longevity. Nature genetics,2003:33(1):40-8.
16. Li S, Kim HE. Implications of sphingolipids on aging and age-related diseases. Frontiers in aging,2022:2:797320.
17. Lynn DA, Dalton HM, Sowa JN, Wang MC, Soukas AA, Curran SP. Omega-3 and-6 fatty acids allocate somatic and germline lipids to ensure fitness during nutrient and oxidative stress in Caenorhabditis elegans. Proceedings of the National Academy of Sciences,2015:112(50):15378-83.
18. Maciej SE. Investigating the role of lipid metabolism in C. elegans mitochondrial isp-1; ctb-1 mutant, 2020.
19. Maglioni S, Mello DF, Schiavi A, Meyer JN, Ventura N. Mitochondrial bioenergetic changes during development as an indicator of C. elegans health-span. Aging (Albany NY),2019:11(16):6535.
20. Mao K, Ji F, Breen P, Sewell A, Han M, Sadreyev R, *et al*. Mitochondrial dysfunction in C. elegans activates mitochondrial relocalization and nuclear hormone receptor-dependent detoxification genes. Cell metabolism,2019:29(5):1182-91.
21. Murphy CT, McCarroll SA, Bargmann CI, Fraser A, Kamath RS, Ahringer J, *et al*. Genes that act downstream of DAF-16 to influence the lifespan of Caenorhabditis elegans. Nature,2003:424(6946):277-83.
22. Rana A, Oliveira MP, Khamoui AV, Aparicio R, Rera M, Rossiter HB, *et al*. Promoting Drp1-mediated mitochondrial fission in midlife prolongs healthy lifespan of Drosophila melanogaster. Nature communications,2017:8(1):448.
23. Rufini A, Tucci P, Celardo I, Melino G. Senescence and aging: the critical roles of p53. Oncogene,2013:32(43):5129-43.
24. Schindelin J, Arganda-Carreras I, Frise E, Kaynig V, Longair M, Pietzsch T, *et al*. Fiji: an open-source platform for biological-image analysis. Nature methods,2012:9(7):676-82.
25. Spinelli JB, Haigis MC. The multifaceted contributions of mitochondria to cellular metabolism. Nature cell biology,2018:20(7):745-54.
26. Staab TA, McIntyre G, Wang L, Radeny J, Bettcher L, Guillen M, *et al*. The lipidomes of C. elegans with mutations in asm-3/acid sphingomyelinase and hyl-2/ceramide synthase show distinct lipid profiles during aging. Aging (Albany NY),2023:15(3):650.
27. Stuhr NL, Nhan JD, Hammerquist AM, Van Camp B, Reoyo D, Curran SP. Rapid lipid quantification in Caenorhabditis elegans by oil red O and Nile red staining. Bio-protocol,2022:12(5):e4340-.
28. Sun N, Youle RJ, Finkel T. The mitochondrial basis of aging. Molecular cell,2016:61(5):654-66.
29. Torgovnick A, Schiavi A, Testi R, Ventura N. A role for p53 in mitochondrial stress response control of longevity in C. elegans. Experimental gerontology,2010:45(7-8):550-7.
30. Ventura N, Rea SL, Schiavi A, Torgovnick A, Testi R, Johnson TE. p53/CEP-1 increases or decreases lifespan, depending on level of mitochondrial bioenergetic stress. Aging cell,2009:8(4):380-93.
31. Walter L, Baruah A, Chang HW, Pace HM, Lee SS. The homeobox protein CEH-23 mediates prolonged longevity in response to impaired mitochondrial electron transport chain in C. elegans. PLoS biology,2011:9(6):e1001084.
32. Wang W, Sherry T, Cheng X, Fan Q, Cornell R, Liu J, *et al*. An intestinal sphingolipid confers intergenerational neuroprotection. Nature Cell Biology,2023:25(8):1196-207.
33. Wang Y, Oxer D, Hekimi S. Mitochondrial function and lifespan of mice with controlled ubiquinone biosynthesis. Nature communications,2015:6(1):6393.
34. West AP, Shadel GS. Mitochondrial DNA in innate immune responses and inflammatory pathology. Nature Reviews Immunology,2017:17(6):363-75.
35. Xu C, Hwang W, Jeong DE, Ryu Y, Ha CM, Lee SJ, *et al*. Genetic inhibition of an ATP synthase subunit extends lifespan in C. elegans. Scientific reports,2018:8(1):14836.
36. Yang W, Hekimi S. Two modes of mitochondrial dysfunction lead independently to lifespan extension in Caenorhabditis elegans. Aging cell,2010:9(3):433-47.
37. Yu FP, Amintas S, Levade T, Medin JA. Acid ceramidase deficiency: Farber disease and SMA-PME. Orphanet journal of rare diseases,2018:13(1):121.
38. Zhi D, Zhao C, Dong J, Ma W, Xu S, Yue J, *et al*. cep-1 mediated the mitohormesis effect of Shengmai formula in regulating Caenorhabditis elegans lifespan. Biomedicine & Pharmacotherapy,2022:152:113246.